Molecular Crystals and Liquid Crystals

Publication details, including instructions for authors and subscription information:
http://www.tandfonline.com/loi/gmcl20

Charge Carrier Trapping in Organic Solar Cell Structures P3HT:PCBM

V. Kažukauskas [a], M. Pranaitis [a], F. Kajzar [b], M. Glatthaar [c] & A. Hinsch [c]

[a] Semiconductor Physics Department, Institute of Materials Science and Applied Research of Vilnius University, Vilnius, Lithuania

[b] University of Angers, Angers, France

[c] Fraunhofer Institute for Solar Energy Systems ISE, Freiburg, Germany

Version of record first published: 22 Sep 2010

To cite this article: V. Kažukauskas, M. Pranaitis, F. Kajzar, M. Glatthaar & A. Hinsch (2008): Charge Carrier Trapping in Organic Solar Cell Structures P3HT:PCBM, Molecular Crystals and Liquid Crystals, 484:1, 373/[739]-381/[747]

To link to this article: http://dx.doi.org/10.1080/15421400801905036

Mol. Cryst. Liq. Cryst., Vol. 484, pp. 373/[739]–381/[747], 2008

ISSN: 1542-1406 print/1563-5287 online
DOI: 10.1080/15421400801905036

Taylor & Francis
Taylor & Francis Group

Charge Carrier Trapping in Organic Solar Cell Structures P3HT:PCBM

V. Kažukauskas[1], M. Pranaitis[1], F. Kajzar[2], M. Glatthaar[3], and A. Hinsch[3]

[1]Semiconductor Physics Department, Institute of Materials Science and Applied Research of Vilnius University, Vilnius, Lithuania
[2]University of Angers, Angers, France
[3]Fraunhofer Institute for Solar Energy Systems ISE, Freiburg, Germany

We have investigated carrier transport and trapping in blends of 6:5 wt. P3HT:PCBM that are important for the development of organic Solar cells. The devices with the inverted layer sequence and solar efficiency of 3.7% were analysed. We demonstrate that, though the fill factor of the IV characteristics is as high as 68%, carrier trapping is effectively involved in the transport phenomena. The evaluated trapping state activation energy is about 0.18 eV and their density is up to $10^{20} \div 7 \times 10^{21}\,cm^{-3}$. At such high density these states may probably act as transport states, limiting carrier mobility. The results were analyzed by taking into account mobility variation according to the Gaussian disorder model as well as carrier thermal generation from traps. The mobility parameters obtained by both methods demonstrate good coincidence.

Keywords: carrier trapping; efficiency; inverted layer sequence; mobility; organic solar cells

PACS numbers: 73.50.-h, 73.61.Ph, 85.60.Bt

1. INTRODUCTION

In photonic organic material engineering and device development carrier transport properties are of primary importance as they are directly related with macroscopic material parameters determining

We acknowledge the partial financial support by the European Commission within the FP6 MOLYCELL project, contract No SES6-CT-2003-502783.

Address correspondence to V. Kažukauskas, Department of Semiconductor Physics and Institute of Materials Science and Applied Research, Vilnius University, Saulėtekio 9, bldg. 3, LT-10222 Vilnius, Lithuania. E-mail: vaidotas.kazukauskas@ff.vu.lt

device functionality and efficiency. Charge carrier mobility is one of the main factors limiting carrier transport in polymers which by their nature are highly disordered [1,2]. On the other hand mobility (at least of one sign carriers in a given material) can often be limited by severe carrier trapping. This results in an imbalance of different carrier flows, and requires specific technological measures to be undertaken to eliminate the problem. Evidence of the charge trapping effects depending on the applied bias to the MDMO-PPV:PCBM bulk-heterojunction Solar cells was evidenced in [3]. Carrier trapping was proven not only in organic devices and blends [2–5], but in single layer samples as well [e.g., 6], evidencing that carrier trapping is an internal feature of organic materials. Therefore fundamental investigations of complex carrier transport phenomena are challenging and practically important task. In this presentation carrier transport and trapping effects will be analyzed in blends of P3HT with PCBM that are of particular importance for the development of Solar cells.

2. SAMPLES AND EXPERIMENT

We had investigated organic bulk-heterojunction Solar cell devices, the active layer of which was formed by the poly-3-hexylthiophene (P3HT) and the fullerene derivative [6,6]-phenyl-C_{61}-butyric acid methyl ester (PCBM). The structures of both constituents are presented in Figure 1. The investigated devices were produced in the so-called inverted layer sequence, that offers some advantages as compared to the devices of conventional setup [7]. Device layout is presented in Figure 2. The devices were fabricated on a cleaned floatglass. First an Al layer of 80 nm was thermally evaporated, then a Ti layer of 20 nm was evaporated by electron-beam heating, both in vacuum better than 10^{-5} mbar. Ti forms the electron contact, while the Al layer is needed for having a high sheet conductance of the

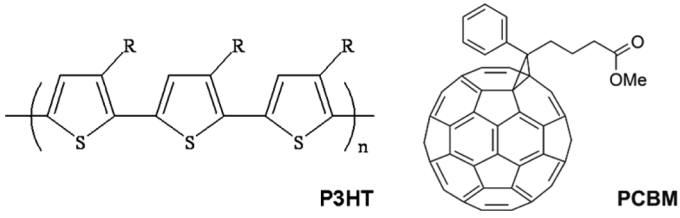

FIGURE 1 Structures of the blend constituents P3HT ($R = C_6H_{13}$) and PCBM.

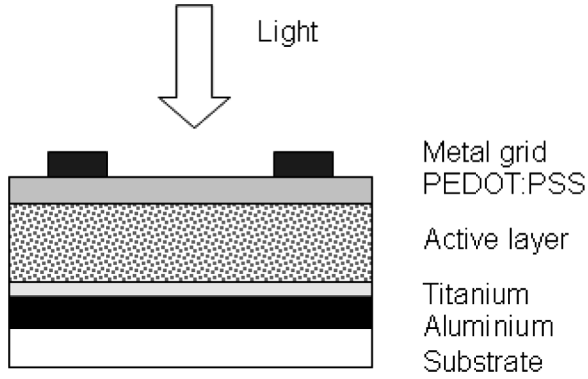

FIGURE 2 The inverted device layout.

electrode. Now the photoactive layer was spin coated from the tetralin solution ($\sim$2% wt.) with a ratio of 6:5 wt. P3HT:PCBM (P3HT 4002 electronic grade synthesized by Rieke Metals, PCBM synthesized by Nano-C). The layer thickness was about 200 nm. As a hole contact PEDOT:PSS was spincoated on top (Baytron F CPP105D) with a layer thickness of 200 nm. To support the sheet conductance of the PEDOT:PSS layer a gold grid was evaporated upon it with a finger width of 100 μm and a distance between the fingers of 500 μm. After the preparation the samples have been annealed for 10 min at 100°C.

Current-Voltage characterization was used to investigate carrier injection properties. Carrier traps were analyzed by the Thermally Stimulated Current (TSC) spectroscopy [6], and carrier mobility measurements were performed by the CELIV (Charge Extraction by Linearly Increasing Voltage) method [8].

The experimental results were analyzed numerically by taking into account mobility variation according to the Gaussian Disorder Model (GDM) approximation [9] as well as carrier thermal generation from traps [10,11]. Such complex analysis had enabled not only evaluation of the trap parameters, but it had also demonstrated a clear coincidence of the results given by both methods, evidencing that carrier trapping is a decisive factor, giving their mobility behaviour.

3. RESULTS AND DISCUSSION

3.1. Solar Cell Performance

To test the quality of the devices IV curves were measured under illumination by AM 1.5 spectrum light with 100 mW/cm^2 incident

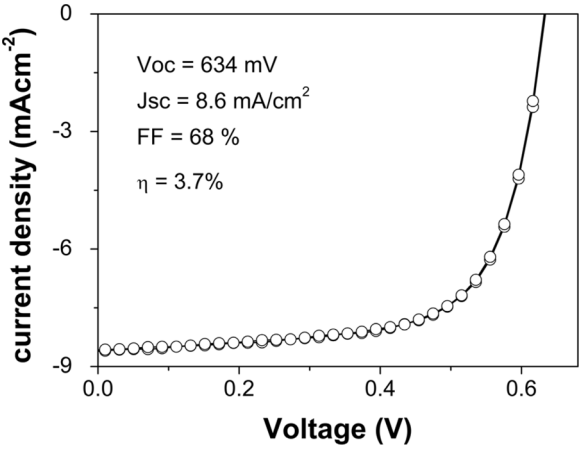

FIGURE 3 Current-density versus voltage under illumination by AM 1.5 spectrum light with 100 mW/cm^2 power density.

power density. A typical curve is presented in Figure 3. In the tested devices a solar efficiency of $(3.7 \pm 0.2)\%$ was reached. The high fill factor of 68%, the open circuit voltage of 634 mV and the short circuit current of 8.6 mA/cm^2 demonstrate significant improvement of the device parameters as compared to the first devices produced in this layout [7]. Moreover the high fill factor evidences that transport problems are of minor importance. Nevertheless to have a clearer insight, we had investigated carrier transport properties in more detail as described below.

3.2. Carrier Trapping

The experimental TSC spectra are presented in Figures 4 (a) and (b) for two devices fabricated on the same glass substrate. Notably, though the devices were produced simultaneously, their current spectra do not coincide quantitatively, indicating that even small variations in technological process might result in significant deviations of device properties. Nevertheless, upon subtraction of the dark current from the TSCs obtained after the light excitation, a qualitative coincidence of the results is clearly seen. In both cases characteristic maxima appear in the TSC curves, which, though being different in detail, demonstrate qualitative similarity. Appearance of the current maxima cannot be explained by carrier mobility behaviour within the predominant GDM approximation, which foresees only mobility increase with

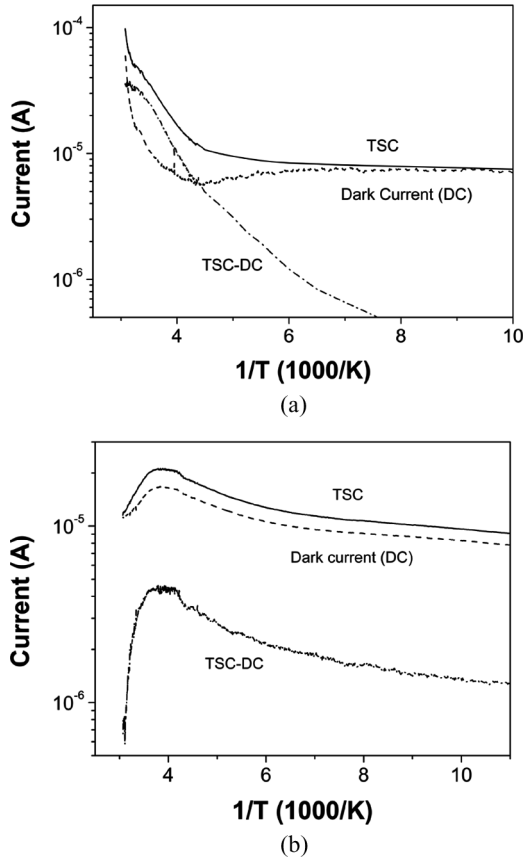

FIGURE 4 Experimental spectra of the TSCs measured after excitation (solid curves), dark currents (dashed curves) and their differences (dashed-dotted curves) in two samples (a and b).

temperature. Though in systems with two perfectly blocking electrodes current maxima can appear when, because of the growing mobility, all carriers become extracted from the device [12]. In such case maxima positions should demonstrate an expressed dependence on the heating rate and applied electric field [12], and we did not observe such behavior. Moreover in our samples current growth took place after the maxima were passed, indicating that the TSC maxima were caused by the emptying of the trapping states.

Therefore the obtained resulting curves were modelled by taking into account the carrier mobility increase and thermal generation of

carriers from trap states as it was described in detail in [6]. The results for the same samples are presented in Figures 5 (a) and (b). The thermal activation energy values of the traps were coinciding well within the range of experimental errors: they were equal 0.18 ± 0.02 eV in all samples. The density of traps was evaluated by integrating the current dependence over time. It was found to range between $10^{20}\,\mathrm{cm}^{-3}$ to some $10^{21}\,\mathrm{cm}^{-3}$. Such high density of the traps implies that they could take active part in carrier transport, acting as transport states and mediating carrier hopping. Qualitatively similar effect called impurity band transport is well known in crystalline semiconductors. Characteristically in samples of lower conductivity trap density was

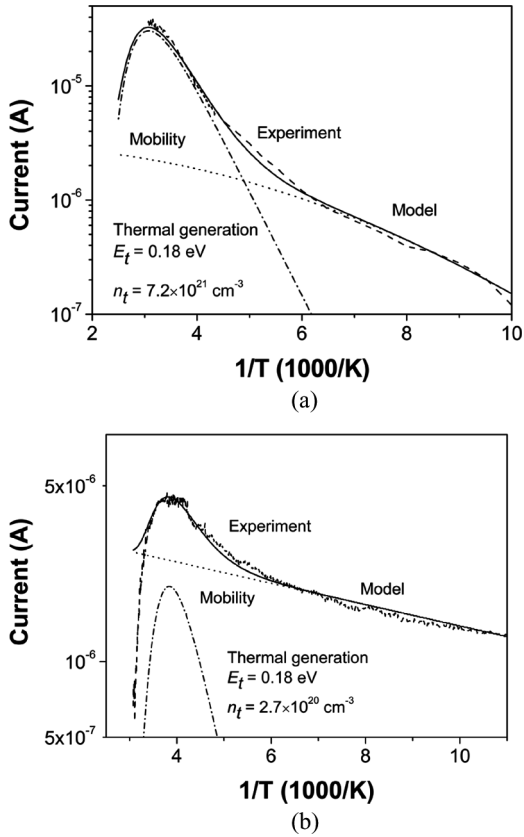

FIGURE 5 Experimental curves (dashed curves) and their modelling (solid curves) by taking into account carrier mobility variation (dotted lines) and thermal generation of carriers (dash-dotted curves) in two samples (a and b).

also significantly lower [4,6], confirming qualitatively the above conclusion. The coinciding activation energy of the traps in different samples and their high density imply that they are most probably not caused by the dopants, e.g., oxygen, but are rather related to material structure itself.

3.3. Mobility Behaviour

Carrier mobility data could be compared by two different methods: TSCs and direct mobility measurements, the results of which are presented in Figure 6. In GDM charge transport in disordered organic conductors is supposed to proceed by means of hopping in a Gaussian site-energy distribution, reflecting the energetic spread in the charge transporting levels of chain segments due to fluctuation in conjugation lengths and structural disorder [9]:

$$\mu(F,T) = \mu_\infty \exp\left[-\left(\frac{2\sigma}{3kT}\right)^2\right] \exp\left\{C\left[\left(\frac{\sigma}{kT}\right)^2 - \Sigma^2\right]\sqrt{F}\right\}. \qquad (1)$$

This Equation was derived from Monte-Carlo simulations of the hopping processes of charge carriers in a material with energetic (σ) and positional disorder (Σ) described by Gaussian distribution functions. μ_∞ is the high temperature limit of the mobility and C is a specific parameter that is obtained from the simulations as $C = 2.9 \times 10^{-4}\,(\mathrm{cm/V})^{1/2}$. Fitting of the TSCs by GDM, shown in Figures 5 (a)

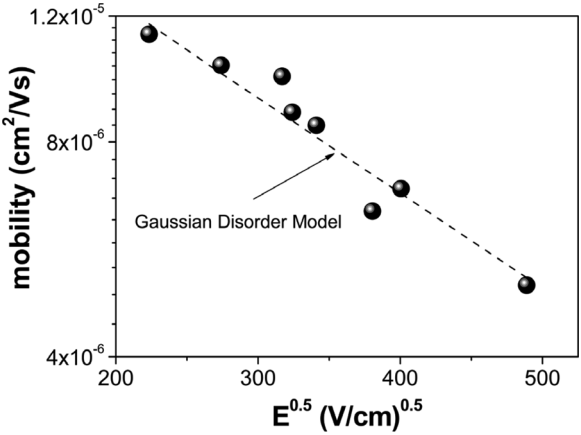

FIGURE 6 Mobility dependence versus applied electric field strength and its fitting by the Gaussian Disorder Model.

and (b) by dotted lines, have given the following values: the positional disorder parameter Σ was equal to 4.5, and the parameter of energetic disorder σ ranged from 0.028 to 0.042 eV. The high-temperature mobility limit μ_∞ was found to be $(1.5 \div 1.9) \times 10^{-3}\,\mathrm{cm}^2/\mathrm{Vs}$, meanwhile coefficient C was $(4.5 \div 6) \times 10^{-4}\,(\mathrm{cm/V})^{0.5}$.

The so-called negative mobility behaviour was observed in Figure 6. Such behaviour is usually observed in materials in which carrier transport is governed by the positional disorder, rather than the energetic one. Similar behaviour was many times observed in different disordered materials as, e.g., molecularly doped polymers, molecular glasses, etc. In polymers, the negative mobility behaviour was first evidenced by the CELIV method in P3HT in [13] and P3OT in [14]. The prevailing role of positional disorder is quite logical in the investigated Solar cells with bulk heterojunction structure in which existence of the positional disorder is the necessary condition for the high efficiency. The experimentally measured dependence in Figure 6 was also fitted by the GDM with the following fitting parameters: $\Sigma = 4.5$, $\sigma = 0.045\,\mathrm{eV}$, $\mu_\infty = 9.5 \times 10^{-4}\,\mathrm{cm}^2/\mathrm{Vs}$, $\mathrm{C} = 1.8 \times 10^{-4}\,(\mathrm{cm/V})^{0.5}$. It can be seen that the fitting parameters of the experimental data obtained by completely different methods coincide quite well. This evidences that carrier trapping is a decisive factor, giving their mobility behaviour.

SUMMARY AND CONCLUSIONS

Carrier transport and trapping effects were analyzed in bulk-heterojunction structures of P3HT and PCBM that are of particular importance for the development of organic Solar cells. The samples were produced from 6:5 wt. P3HT:PCBM blends in the inverted layer sequence configuration. First Al layer of 80 nm was evaporated on the floatglass. The Ti layer of 20 nm was evaporated on it to form the electron contact. Afterwards 200 nm thick photoactive layer was spin coated from $\sim 2\%$ wt. tetralin solution. As a hole contact PEDOT:PSS was spin coated on the top with a layer thickness of 200 nm. Finally, to support the sheet conductance of the PEDOT:PSS layer the gold grid was evaporated with a finger width of 100 μm and a distance between the fingers of 500 μm. The samples have been annealed for 10 min at 100°C.

Carrier mobility measurements were performed by the CELIV method, carrier traps were analyzed by the Thermally Stimulated Current spectroscopy, and Current-Voltage characterization was used to investigate carrier injection properties. The energy conversion

efficiency of the devices was 3.7% and the fill factor of the IV characteristics was up to 68%. Despite such relatively good parameters, carrier trapping was demonstrated to be effectively involved in the transport phenomena. The evaluated trapping state activation energy was about 0.18 eV and their density reached up to $10^{20} \div 7 \times 10^{21}\,\mathrm{cm}^{-3}$. At such high density these states may probably act as transport states, limiting carrier mobility. The results were analyzed numerically by taking into account mobility variation according to the Gaussian disorder model as well as carrier thermal generation from the trap states. The mobility parameters obtained from the TSC and direct mobility measurement methods were coinciding well, thus evidencing that carrier trapping is among the main factors, determining their mobility behaviour.

REFERENCES

[1] Kim, Y., Cook, S., Tuladhar, S. M., Choulis, S. A., Nelson, J., Durrant, J. R., Bradley, D. D. C., Giles, M., Mcculloch, I., Ha, C. S., & Ree, M. (2006). *Nature Mater.*, *5*, 197.
[2] Pacios, R., Chatten, A. J., Kawano, K., Durrant, J. R., Bradley, D. D. C., & Nelson, J. (2006). *Adv. Funct. Mater.*, *16*, 2117.
[3] Offermans, T., Meskers, S. C. J., & Janssen, R. A. J. (2006). *Org. Electron.*, *7*, 213.
[4] Kažukauskas, V., Čyras, V., Pranaitis, M., Apostoluk, A., Rocha, L., Sicot, L., Raimond, P., & Sentein, C. (2007). *Org. Electron.*, *8*, 21.
[5] Renaud, C., Huang, C. H., Zemmouri, M., Le Rendu, P., Nguyen, T. P. (2006). *Eur. Phys. J. Appl. Phys.*, *36*, 215.
[6] Kažukauskas, V. (2004). *Semicond. Sci. Technol.*, *19*, 1373.
[7] Glatthaar, M., Niggemann, M., Zimmermann, B., Lewer, P., Riede, M., Hinsch, A., & Luther, J. (2005). *Thin Solid Films*, *491*, 298.
[8] Juška, G., Arlauskas, K., Viliūnas, M., & Kočka, J. (2000). *Phys. Rev. Lett.*, *84*, 4946.
[9] Baessler, H. (1993). *Phys. Stat. Solidi (b)*, *175*, 15.
[10] Simmons, J. G. & Taylor, G. W. (1972). *Phys. Rev. B*, *5*, 1619.
[11] Kavaliauskienė, G., Kažukauskas, V., Rinkevičius, V., Storasta, J., Vaitkus, J. V., Bates, R., O'Shea, V., & Smith, K. M. (1999). *Appl. Phys. A*, *69*, 415.
[12] Chen, I. (1976). *J. Appl. Phys.*, *47*, 2988.
[13] Mozer, A. J., Sariciftci, N. S., Pivrikas, A., Österbacka, R., Juška, G., Brassat, L., & Bässler, H. (2005). *Phys. Rev. B*, *71*, 035214.
[14] Kažukauskas, V., Pranaitis, M., Sicot, L., & Kajzar, F. (2006). *Mol. Cryst. Liq. Cryst.*, *447*, 459.